Biochimica et Biophysica Acta 1847 (2015) 390–398

Contents lists available at ScienceDirect

Biochimica et Biophysica Acta

journal homepage: www.elsevier.com/locate/bbabio

# Novel expression and characterization of a light driven proton pump archaerhodopsin 4 in a *Halobacterium salinarum* strain

Zhen Cao [a], Xiaoyan Ding [a], Bo Peng [a], Yingchun Zhao [b], Jiandong Ding [b], Anthony Watts [c], Xin Zhao [a,*]

[a] Shanghai Key Laboratory of Magnetic Resonance, Department of Physics, East China Normal University, Shanghai 200062, PR China
[b] State Key Laboratory of Molecular Engineering of Polymers, Department of Macromolecular Science, Fudan University, Shanghai 200433, PR China
[c] Biomembrane Structure Unit, Department of Biochemistry, University of Oxford, South Parks Road, Oxford OX1 3QU, UK

ARTICLE INFO

*Article history:*
Received 15 July 2014
Received in revised form 22 December 2014
Accepted 25 December 2014
Available online 2 January 2015

*Keywords:*
Archaerhodopsin 4
Light-driven proton pump
Expression
Bacterioruberin and trimeric packing
Solid-state NMR

ABSTRACT

Archaerhodopsin 4 (AR4), a new member of the microbial rhodopsin family, is isolated from *Halobacterium species xz515* in a Tibetan salt lake. AR4 functions as a proton pump similar to bacteriorhodopsin (BR) but with an opposite temporal order of proton uptake and release at neutral pH. However, further studies to elucidate the mechanism of the proton pump and photocycle of AR4 have been inhibited due to the difficulty of establishing a suitable system in which to express recombinant AR4 mutants. In this paper, we report a reliable method for expressing recombinant AR4 in *Halobacterium salinarum* L33 with a high yield of up to 20 mg/l. Experimental results show that the recombinant AR4 retains the light-driven proton pump characteristics and photo-cycling kinetics, similar to that in the native membrane. The functional role of bacterioruberin in AR4 and the trimeric packing of AR4 in its native and recombinant forms are investigated through light-induced kinetic measurements, two-dimensional solid-state NMR experiments, dynamic light scattering (DLS) and Fourier transform infrared spectroscopy (FTIR). Such approaches provide new insights into structure–function relationships of AR4, and form a basis for other archaeal rhodopsins.

© 2015 Elsevier B.V. All rights reserved.

## 1. Introduction

Microbial rhodopsins are a large family of photoactive seven-transmembrane retinylidene proteins that include bacteriorhodopsin (BR) [1], archaerhodopsin (AR) [2], halorhodospin (HR) [3], proteorhodopsin (PR) [4], sensory rhodopsin (SR) [5] and xanthorhodopsin (XR) [6]. Comparisons of these retinylidene proteins are critical for deep understanding of the relationship between structure and function, and provide insights into the individual light-driven photocycle. BR was the first discovered microbial rhodopsin in haloarchaea and identified as a light-driven proton pump [7]. It serves as a model for investigating the vectorial ion translocation across membranes [8–11] and a template for G protein-coupled receptors [12], as it is a highly stable protein under experimental conditions [13,14]. Archaerhodopsins (ARs) are also light-driven proton pumps with a high degree of amino acid sequence homology to BR, and exhibit similar photochemical properties [15–18].

Archaerhodopsin 4 (AR4), the only protein found in the claret membrane of *Halobacterium species (H. sp.) xz515*, was collected from a salt lake in Tibet [18–22]. It was named as the fourth archaerhodopsin, as it exhibits 87% sequence similarity to AR1, 97% to AR2 and 84% to AR3. AR4 also shares 59% sequence identity with bacteriorhodopsin [23], but shows a different proton pumping behavior with an opposite temporal order of the light-driven proton release and uptake under physiological conditions [24–26]. The color difference between the claret membrane and purple membrane may be mainly due to the presence of carotenoid bacterioruberin (5,32-bis(2-hydroxypropan-2-yl)-2,8,12,16,21,25,29,35-octamethylhexatriaconta-6,8,10,12,14,16,18,20, 22,24,26,28,30-tridecaene-2,35-diol), and it has been suggested that it plays a role in trimerization of the protein [27]. Since a p$K_a$ value change from 10.4 to 8.4 was reported for the proton release complex (PRC) in AR4, and a p$K_a$ value change from 9.7 to 5.7 for the proton release complex in BR [23], the "weak-coupling model" was proposed to explain the proton transport mechanism of AR4, i.e. the higher p$K_a$ of PRC leads to a temporal alteration in proton release order [22]. Alternation of time sequence of proton pumping by the presence of Triton X-100 or crown ethers at neutral pH has also been reported [24,28]. However, little is known about details of the proton pumping mechanism of AR4 and the other three archaerhodopsins.

Choosing an appropriate host is very important for expressing retinylidene proteins from Archaea (*Halobacterium salinarum* and *H. sp. xz515*) [29], and although many kinds of microbial rhodopsins have been successfully expressed in the plasma membrane of *Escherichia coli* [30–33], there are still some drawbacks for *E. coli* as the host. Firstly, exogenous retinal has to be added during the expression of retinal-binding proteins in *E. coli* [33]. Secondly, the membrane of Archaea is known to contain many unique polar lipids, based on

* Corresponding author. Tel./fax: +86 21 62234329.
*E-mail address:* xzhao@phy.ecnu.edu.cn (X. Zhao).

http://dx.doi.org/10.1016/j.bbabio.2014.12.008
0005-2728/© 2015 Elsevier B.V. All rights reserved.

2,3-dialkyl-*sn*-glycerol backbones, which is entirely different from that of bacteria (*E. coli*) [34]. So *H. salinarum* L33 (*bop*$^-$) might be the most appropriate host for expressing functional recombinant AR4, since both L33 and *H. sp. xz515* are halophilic Archaea.

Here, a new approach has been established to express the functional recombinant AR4 in *H. salinarum* L33 by some novel modifications of the gene at the 5′ end to increase the translational efficiency, so a high expression yield of 20 mg/l has been achieved by the method. Functional assays have shown that the recombinant AR4 retains similar light-driven proton pump characteristics and photo-cycling kinetics of the native protein in the claret membrane. Trimeric packing and dynamic conformation of AR4 in its native and the recombinant forms have been investigated through light-induced kinetic measurements, two-dimensional (2D) solid-state NMR (SSNMR) experiments, dynamic light scattering (DLS), and Fourier transform infrared (FTIR) spectroscopy, respectively. Approaches used here provide new insights into structure–function relationships of AR4, and form a basis for other proteins of the archaeal rhodopsin family.

## 2. Materials and methods

### 2.1. Gene cloning and transformation

Expression vectors were constructed using the shuttle plasmid pXLNovR with *Hin*d III and *Bam*H I restriction sites [35]. The opsin gene of AR4, termed as *ar4*, was amplified from the genome of *H. sp. xz515* [36] and was modified as follows: (i) the entire propeptide nucleotide sequence of *ar4* was replaced by the same part of the *bop* gene, termed as *btar* gene, and (ii) 27 base pairs from the start codon of the *ar4* gene were replaced by the same part of the *bop* gene to construct a chimeric propeptide sequence, termed as the *bar* gene (Fig. 1A). The *ar4* gene together with *btar* and *bar* genes was combined with the promoter of *bop* and subcloned into expression vector to yield pXLNovR-*ar4*, pXLNovR-*bar* and pXLNovR-*btar*. The construction details are provided in the supplementary material (Fig. S1 and Table S1). All the expression vectors were transformed into *H. salinarum* L33 (*bop*$^-$) separately according to the method described by Needleman et al. [35]. The transformants grew on the plates which contained 0.5 μg/ml novobiocin for two weeks under illumination to isolate correct colonies by screening color change. The recombinant colonies were also verified by sequencing. Plasmids were first isolated from a bacterial culture of each group. Then, the insert DNA was identified by sequencing using appropriate primers for the target gene (Primer 1: 5′-CGGGATCCGACGTG AAGA TGGGG-3′; Primer 2: 5′-GCCAAGCTTCTAGATCAGTCGCTG-3′). Finally, a single colony was selected for large-scale culture with the addition of 1 μg/ml novobiocin.

### 2.2. Culturing and isolation

Culture and isolation of native AR4 in the claret membrane of *H. sp. xz515* have been reported by Ming et al. [23]. Briefly, a starting culture of 25 ml from a single colony was incubated for every 500 ml culture. A sucrose gradient with concentrations of 30%, 35%, 40% and 45% (w/w) was used for purification of the claret membrane by centrifugation. After 12 h of centrifugation at 35,000 rpm and 15 °C (rotor SW41, Beckman, USA), the portion was collected from the 40% sucrose layer and washed with deionized water for three times and then kept for later use. The recombinant AR4 was prepared by growing the screened L33, a standard procedure for culture and isolation of purple membrane was used [37] with a slight modification. Briefly, a 25 ml starting culture incubated with a single colony was prepared for every 500 ml culture. The cell culture was performed either in complete or synthetic medium [38]. [U-$^{13}C_9$,$^{15}$N]-Leu labeled native AR4 and recombinant AR4 were prepared by growing *xz515* and L33 in synthetic medium separately, in which the unlabeled Leu was replaced by isotope-labeled Leu. The sucrose density gradient for the purification of recombinant AR4 was, from the bottom, 60%, 43% and 35% (w/w). After centrifugation (25,000 rpm, 15 °C, 15 h, rotor JA-30.50 Ti, Beckman, USA), the sample was removed from the 43% sucrose layer and washed in deionized water.

### 2.3. Light-induced kinetic measurements

The proton pumping activities of the native and recombinant AR4 proteins were monitored through a light-induced absorption change by a pH-sensitive dye, pyranine (8-hydroxy-1,3,6-pyrenetrisulfonic acid, trisodium salt) on a homemade apparatus as described previously [18,23,39]. The net proton pumping activity was determined by taking the absorbance difference at 456 nm before and after adding the dye. The kinetics of M-state, O-state and recovery trajectory to the ground state were monitored at 410 nm, 660 nm and 570 nm, respectively. All the experiments were carried out by using a camera photoflash with the half-bandwidth less than 1 ms for excitation. All the samples were in light adapted conformation and suspended in a buffer with 100 mM NaCl and 20 mM KCl at pH 7.0. All the measurements were performed at room temperature.

### 2.4. Solid-state NMR experiments

Solid-state NMR measurements were carried out on a Bruker Avance III 600 MHz wide bore spectrometer using either a 4 mm HXY MAS probe or a 3.2 mm HCN Efree MAS probe. All the experiments were performed at a MAS speed of 8000 ± 5 Hz regulated by a Bruker MAS

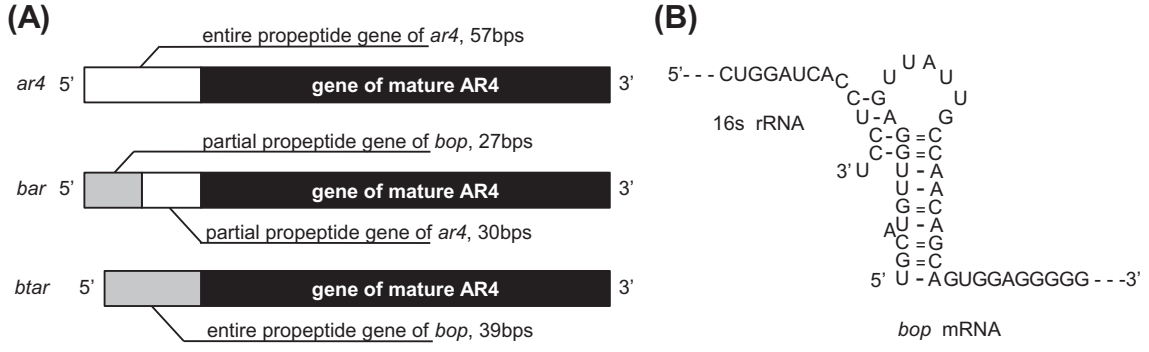


**Fig. 1.** Three types of genes designed for the expression of recombinant AR4 (A). The hairpin structure at the 5′ end of *bop* mRNA and its complementary to the 3′ end of *H. salinarum* 16s rRNA (B).

controller, and the temperature was controlled at −20 ± 1 °C under dark condition. In all experiments, a ramped cross-polarization (CP) [40,41] was used with a radio frequency (rf) field of 50 kHz on the proton channel. Typical 90° rf pulse lengths of 4 μs for $^{13}C$ and 3.5 μs for $^{1}H$ channels, and the two-pulse phase modulation (TPPM) [42] with a pulse width of 6.5–7 μs for proton decoupling were used throughout the experiments. The $^{13}C$ chemical shifts were referred to the methylene peak of adamantine [43].

Two-dimensional (2D) $^{13}C$–$^{13}C$ correlation spectra of AR4-xz515 and *b*AR were recorded with a 100 ms mixing time by using proton-driven spin-diffusion (PDSD) or dipolar-assisted rotational resonance (DARR) schemes [44,45]. Acquisition times of 20 ms and 5 ms were used in the direct and indirect dimensions, respectively. In the 2D $^{13}C$–$^{13}C$ double-quantum single-quantum (DQ/SQ) correlation experiments, the Post-C7 sequence was used at a rf field of 56 kHz for double quantum excitation and reconversion [46,47]. A continuous wave decoupling at the Lee–Goldburg condition (CWLG) [48] of 85 kHz was applied during the Post-C7 sequence. 2D $^{13}C$–$^{15}N$ correlation experiments was also performed by double-cp (DCP) sequence [49] with a 5 ms mixing time for N–C polarization transfer and a rf power of 46 kHz on the carbon channel. A recycle delay of 3 s was set for all the experiments.

### 2.5. FTIR experiments

FTIR measurements were carried out by using a Nicolet 8700 USB IR spectrometer equipped with a DTGS detector from 4000 to 1000 $cm^{-1}$ wavenumbers. Approximately 50 μg of each protein sample, suspended in 2 mM PBS buffer at pH 7.0, was deposited on $CaF_2$ windows and incubated in a vacuum desiccator for 1 h. Samples were then sealed and mounted on a variable temperature cell. 128 scans with a 4 $cm^{-1}$ resolution were taken for each measurement. Data was processed by the OMNIC 8.1 soft package (Thermo Fisher Scientific Inc.). All experiments were performed at room temperature.

### 2.6. Dynamic light scattering measurements

Average particle sizes and polydispersity indices of the proteins were determined by a dynamic light scattering spectrometer (Malvern Zetasizer Nano ZS90, Malvern Instruments, Malvern, UK) at 20 °C. Samples were diluted with deionized water at pH 7.0 and adjusted to a concentration of 5 μM.

## 3. Results

### 3.1. Expression of recombinant AR4

Three recombinant plasmids, pXLNovR-*ar4*, pXLNovR-*btar* and pXLNovR-*bar*, were transformed into *H. salinarum* L33. As a control, the blank plasmid, pXLNovR, was also transformed into L33. Since the host L33 is colorless, recovery of color was used to screen the correct colonies. Only the colonies which contained the pXLNovR-*bar* plasmid displayed a faint red color, as shown in Fig. S2. Transformations of pXLNovR-*ar4* and pXLNovR-*btar* in L33 still were colorless, as was the control group of pXLNovR. For a further assay, a single colony was picked up from each plate and cultured in 20 ml complete medium under illumination for plasmid extraction. 10 ml of each culture was then centrifuged and only the pellet from the pXLNovR-*bar* group was red (Fig. S3). Sequence of the inserted DNA in each extracted plasmid was also verified, and the results indicated that each recombinant colony contained the correct target gene (Figs. S5–S7), so the single colonies from the pXLNovR-*bar* plate were picked up for further expression and purification, and the purplish-red product was termed as *b*AR (Fig. 2A). Stimulation of L33 cell growth by glucose (Glc) was studied through parallel tests in three 500 ml of synthetic media of 0%, 1% and 2% glucose (w/v), respectively. As a result, the culture which contained 2% glucose gave the highest optical density ($OD_{660\ nm}$) (Fig. 3), consistent with previous work [50]. The final yields for each culture were 18 mg/l (0% Glc), 32.9 mg/l (1% Glc) and 35.5 mg/l (2% Glc). The protein concentration was determined using the Bradford method [51,52].

### 3.2. Assessments of recombinant AR4

The molecular weight of *b*AR, the recombinant AR4, was determined by SDS-PAGE, indicating a similar weight as AR4-xz515, the native protein in the claret membrane of *H. sp. xz515*, as shown in Fig. 2B. The retinal binding in *b*AR was examined through UV–VIS absorption spectroscopy, showing a single absorption peak pattern at about 550 nm (Fig. 2C), similar to the retinal binding in BR [37]. However, the UV–VIS spectrum of AR4-xz515 shows a three peak pattern at 478 nm, 507 nm and 543 nm, respectively, which has been attributed to the presence of a C50-carotenoid lipid in the claret membrane, named as bacterioruberin [18]. Clearly, bacterioruberin is absent in the *b*AR membrane and the UV–VIS spectrum is similar to the bacterioruberin-excluded AR4-xz515, as reported before [18]. A small blue shift in *b*AR when compared with BR may indicate that a slightly different protein packing, which may affect the retinal binding pocket

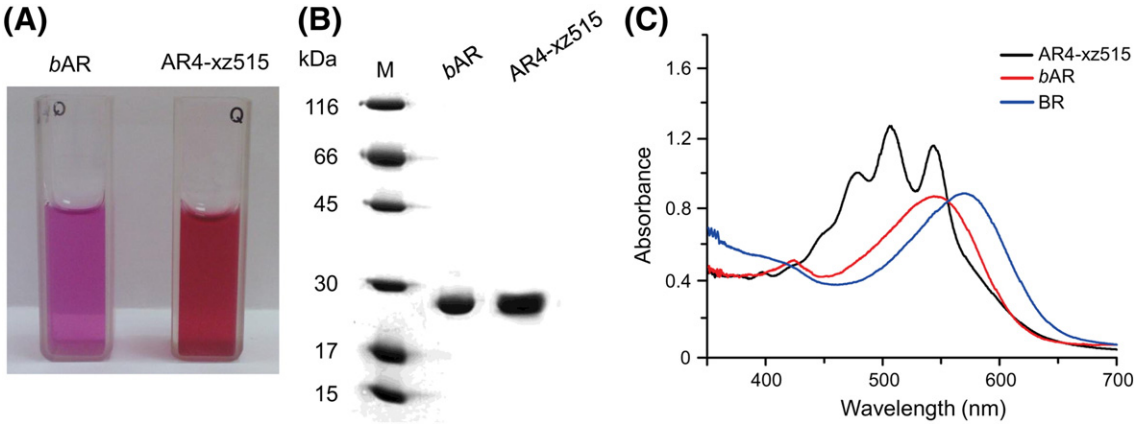


**Fig. 2.** The purplish red membrane from transformed L33 with *bar* gene (*b*AR) and claret membrane from *H. sp. xz515* (AR4-xz515). The concentration of two samples were adjusted to $OD_{550\ nm} = 2.0$ separately (A). The purified AR4 from *H. sp. xz515* and BAR from *H. salinarum* L33 were analyzed by 12% SDS-PAGE. All samples were solubilized in loading buffer containing 3% SDS without preheating (B). The UV–Vis absorption spectra of BR, AR4-xz515 and *b*AR samples were suspended at 100 mM NaCl and 20 mM KCl at pH 7.0 (dark-adapted) (C).

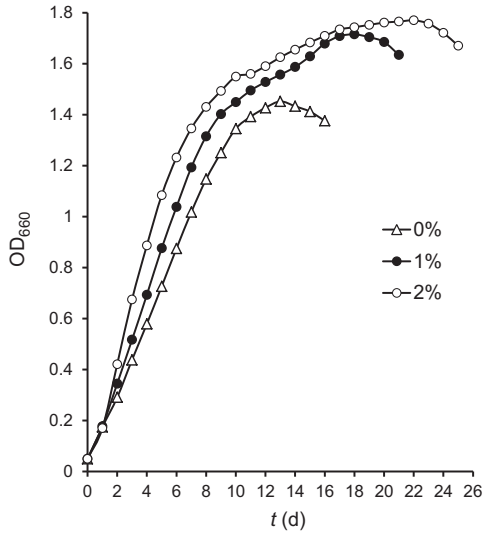


**Fig. 3.** Effect of glucose on growth of *H. salinarum* L33, pXLNovR-*bar* included in synthetic medium. Glucose concentrations are indicated as 0%, 1% and 2% (w/v).

in *b*AR [53], and hydrophobic binding pocket in rhodopsin has also been shown to be functionally important [54]. It is also worth noticing that most members of the *Halobacteriaceae*, including *H. salinarum*, possess bacterioruberin [55,56], whereas no bacterioruberin is present in the purple membrane of *H. salinarum*. Yoshimura and Kouyama [27] has postulated a lipid-recognition mechanism to explain why bacterioruberin is excluded from purple membranes, and this may also explain why bacterioruberin is absent in the recombinant AR4 membrane in *H. salinarum*.

Light-induced proton release and uptake in *b*AR were detected through observing the absorbance change of the dye of pyranine [18,39,57]. An increase in absorbance of pyranine at 456 nm indicates proton uptake by the protein (an alkaline environment), whereas a decrease at 456 nm corresponds to proton release into the medium (an acidic environment). For a comparison, similar experiments were also done on BR and AR4-*xz515*, as showed in Fig. 4, where it is showed that AR4 and BR have a reversed temporal order for proton release and uptake, and *b*AR shows a similar temporal order as AR4-xz515, which indicates that the recombinant AR4 expressed in L33 retains the same proton pumping features as AR4 in the claret membrane of *H. sp. xz515*.

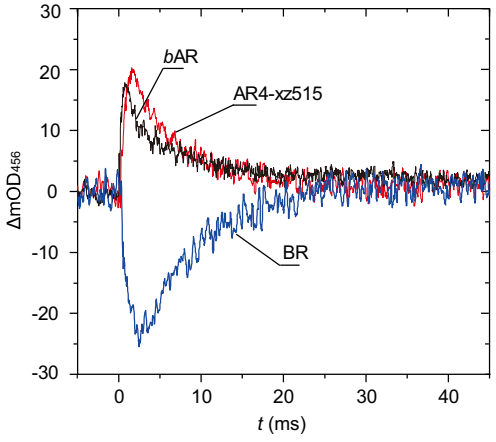


**Fig. 4.** Proton pump behavior of BR, AR4-xz515 and BAR at pH 7.0 in 100 mM NaCl and 20 mM KCl. The pH sensitive dye pyranine is used to measure the transient change of medium pH, indicating the temporal order of proton release and uptake of these proteins after photoexcitation.

The photo-kinetics of M-state, O-state and the recovery trajectory to ground state of AR4 were monitored at 410 nm, 660 nm and 570 nm, respectively (Fig. 5). The measurements suggest that *b*AR has a complete photocycle procedure, similar to that of AR4-xz515. Detailed analysis of the kinetic processes demonstrates that *b*AR and AR4-xz515 have very similar M-state decay, but the decay constants are about 3 times faster than in BR, as shown in Table 1. AR4-xz515 and *b*AR share a close similarity to the formation and decay of the O-intermediate. The recovery trajectory to the ground state of AR4-xz515 and *b*AR could be fitted by a complete exponential curve with a similar decay constant, while BR fits by a single exponential function, which may indicate that AR4 has a more complicated proton transfer mechanism.

Solid-state NMR, FTIR and DLS have also been employed for the assessments of recombinant AR4. Fig. 6A–B shows the 2D DARR and DQ/SQ $^{13}C$–$^{13}C$ correlation experiments on [$^{13}C_9$,$^{15}N$]-Leu labeled native AR4 (black) and recombinant AR4 (red). Essentially all $^{13}C$ atoms within certain distances could be correlated to each other by a longer DARR mixing time through spin diffusion, as can be seen by the cross peaks in the DARR 2D contour map (Fig. 6A), but would be very crowded and cause ambiguity for the peak assignments. This situation could be alleviated with the assistance of the 2D DQ/SQ correlation experiments, since only one bond correlation could be established through C7-type of the symmetry-based homonuclear recoupling sequences [47,58–61], as shown in Fig. 6B. The 2D DQ/SQ correlation experiments would not only simplify the crowded 2D spectra, but also remove all the isolated $^{13}C$ signals from natural abundant contributions from the protein and the associated lipids. Combining these two types of homonuclear correlation experiments together with the N–C type of heteronuclear correlation experiments, an almost completely full assignment of a membrane protein could be achieved [62]. Fig. 6C is a $^{13}C$–$^{15}N$ DCP correlation experiment on [$^{13}C_9$,$^{15}N$]-Leu labeled native AR4 (black) and recombinant AR4 (red). The chemical shifts of the backbone $^{13}CO$, $^{13}CA$ and $^{15}N$ for the recombinant AR4 are all in the ranges typical for a well formed α-helical structure, and in a good agreement with chemical shifts of Leu residues in BR and other retinal proteins by both solution NMR and solid-state NMR [63–66]. Spinning sidebands from the CO peaks in all the $^{13}C$–$^{13}C$ correlation experiments of AR4 clearly indicate that AR4 has a relative rigid transmembrane domain than that of recombinant AR4 which may attribute to the effect of bacterioruberin on the native AR4, as shown by the projections for both $t_1$ and $t_2$ dimensions to the 2D spectra in Fig. 6A–B of $^{13}C$-Leu labeled AR4 (the spinning sidebands are indicated with red stars). This observation is further verified by the $^{13}C$–$^{15}N$ DCP correlation experiments on the native AR4 and recombinant AR4 (Fig. 6C). Evident up-field shifts of all backbone $^{15}N$ in the recombinant AR4 suggest a less compact transmembrane domain than that of in the native AR4. Again, this result also proves that bacterioruberin may interact with the transmembrane helices in the native AR4, which has been shown by the bacterioruberin contained crystal structure of AR2 [27]. Slightly up-field shifted CO and CA peaks in the 2D DQ/SQ $^{13}C$–$^{13}C$ correlation spectra of BR (Fig. 6B) may be attributed to that some mobile Leu residues exist in the protein, and this has been shown in the X-ray crystal structure of BR which shows that there is a Leu residue located at loop region [67,68]. The 2D DQ/SQ $^{13}C$–$^{13}C$ correlation spectra of the $^{13}C$ leu labeled native and recombinant AR4 also show slightly up-field shifted CO and CA peaks, which may indicate the proteins may have a similar structural feature. Our results further demonstrate that this expression method can provide a platform for the structure determination and functional analysis of AR4 by solid-state NMR [66,69–76].

The FTIR spectra of *b*AR and AR4-xz515 are very similar to each other, and also similar to BR, as shown in Fig. 7. All the stretching modes for the amide A and O–H at 3296 $cm^{-1}$, amide I for the backbone C═O and C–N stretching at 1658 $cm^{-1}$, amide II at 1546 $cm^{-1}$ are all showing that the recombinant AR4 has a native well-folded protein secondary structure [77–79]. The bands at 1168 and 1064 $cm^{-1}$ are the typical ethylenic C═C stretching from the retinal chromophore [77,78].

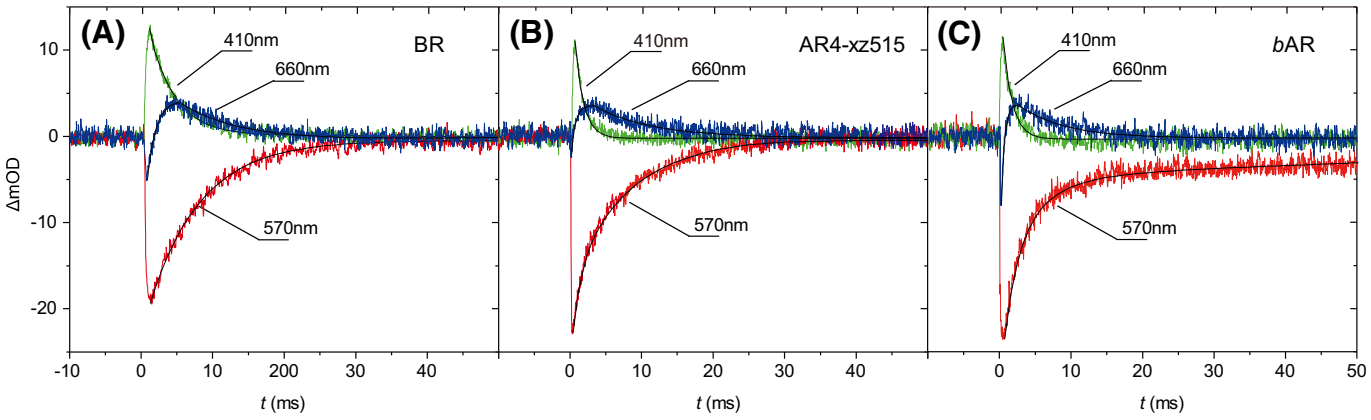


**Fig. 5.** Transient absorption changes of BR (A), AR4-xz515 (B) and *b*AR (C) at the wavelengths indicated (100 mM NaCl and 20 mM KCl, pH 7.0, 25 °C). 410 nm curves represent the formation and decay of the M-state. The recovery of initial state is monitored at 570 nm. Kinetics of O-state formation and decay are detected by the absorbance changes at 660 nm. The smooth black lines through the data represent the results of single or multi-exponential fitting.

It has been reported that only a protein-containing membrane fragment, not the full band, is obtained after standard purification [37]. The particle sizes of native and recombinant AR4 obtained from DLS are listed in Table 2, with the polydispersity indices for the claret membrane and L33 membrane fragments, respectively. The listed value is an average of the nine sets of data. Both the membrane fragments show a single-peak distribution pattern with a narrower band for the claret membrane, suggesting that native AR4 is more compactly packed in the claret membrane than in recombinant AR4 in the L33 membrane, as shown in Fig. 8 and Table 2.

In summary, two-dimensional solid-state NMR experiments, FTIR and DLS measurements clearly show that the recombinant AR4 has the expected protein folding, a functioning retinal chromophore and a similar trimeric packing, similar to the native AR4.

## 4. Discussion

### 4.1. Expression of recombinant AR4

Expression of recombinant AR4 in *H. salinarum* (*bop*$^-$) has been difficult [80], although several other retinal proteins from halophilic bacteria have been reported to express successfully in the same host [81,82]. Here, three plasmids, pXLNovR-*ar4*, pXLNovR-*btar* and pXLNovR-*bar* have been constructed and transformed into *bop*$^-$ strain L33, but only pXLNovR-*bar* is able to express the target protein, indicating that the mosaic propeptide sequence in the *bar* gene may play a key role for the successful expression in L33. According to the analysis of bacteriorhodopsin mRNA, the 5′ terminus contains only three nucleotides beyond the initiator codon, and this terminus could form a hairpin structure [83]. Immediately downstream from the structure, there is a sequence complementary to the 16s rRNA of *H. salinarum* at the 3′ end (Fig. 1B) [83,84]. These features stabilize the mRNA and enhance the translational efficiency [83]. Furthermore, AR4 has a propeptide with 19 residues and hydrophobic tendency, which may direct the newly synthesized protein to cross the membrane [85]. The nucleotide sequence of the propeptide of the *bar* gene is derived from that of *bop* and *ar4* (Fig. 1A and Table S1). Thus, the *b*AR mRNA could form a hairpin structure like that in BR mRNA which consequently facilitates its translation. Additionally, the mosaic propeptide sequence of *bar* can be translated as a peptide of 19 amino acids with hydrophobic tendency. In contrast, the mRNA of *ar4* could not form the hairpin at its 5′ terminus, and the propeptide (13 residues) translated from mRNA of *btar* is too short to assist the folding of the recombinant AR4 in the L33 membrane.

It has been mentioned that *H. salinarum* species are incapable of degradation of sugars [86,87], however, our results demonstrate that the exogenous addition of glucose not only stimulates the cell growth as described previously by Gochnauer and Kushner in 1969 [50], but also increases the yield of recombinant AR4 in the synthetic medium, although the mechanism is still unclear and needs further investigation.

**Table 1**
Time constants and amplitudes resulting from single and multi-exponential fitting to the data traces depicted in Fig. 5[a].

| Sample | M-decay (ms) | O-rise (ms) | O-decay (ms) | Recovery to G state | | |
|---|---|---|---|---|---|---|
| | | | | 1 | 2 | 3 |
| BR | 4.2 | 0.95 | 7.94 | 7.33 | | |
| | 100% | −100% | 100% | −100% | | |
| AR4 | 1.51 | 0.48 | 7.87 | 1.29 | 4.28 | 12.4 |
| | 100% | −100% | 100% | −33% | −28.2% | −38.8% |
| *b*AR | 1.63 | 0.44 | 6.39 | 1.85 | 5.06 | 208 |
| | 100% | −100% | 100% | −43% | −31.4% | −25.6% |

[a] Negative amplitude of exponentials correspond to transient rise in absorbance.

### 4.2. Characterization of recombinant AR4

The steady-state absorption spectrum of AR4 in the claret membrane is shielded by bacterioruberin, which results in unclear on absorption maximum of pure AR4. In previous work [25], the $\lambda_{max}$ of native AR4 was suggested to be 560 nm according to the difference spectra of the claret membrane before and after being bleached by the hydroxylamine. Here, the $\lambda_{max}$ of *b*AR is at 550 nm, which shows blue-shift compared to both AR4-xz515 and BR ($\lambda_{max}$ = 568 nm). According to the mechanism proposed by Wang et al. [53], the bathochromic shifting of retinylidene protein depends on a more evenly dispersed electrostatic potential across the entire polyene chain, which refers to a less compact environment in retinal binding-pocket. Analogously, a 10 nm shift in the absorption spectrum of recombinant AR4 is supposed to be caused by the different protein–chromophore interactions, resulting from the absence of bacterioruberin.

It has been reported that AR4 assembles in a trimer form in the claret membranes revealed by the result of atomic force microscope (AFM) [88]. The results of DLS suggest that *b*AR proteins assemble into stable protein–lipid complexes with similar particle size to the claret membrane fragments (Fig. 8). Although there is currently no direct evidence to reveal the assembly process for recombinant AR4 in the L33 membrane, it may probably be in a trimer form. Wang et al. have reported [89] that monomeric AR4, produced by solubilizing the claret membrane with Triton X-100, exhibited a reversed time order of proton pumping compared to trimeric AR4, whereas the *b*AR retains the native temporal order of proton release and uptake (Fig. 4). In addition, the AR4 monomers displayed a slower M-decay than the AR4 trimers at

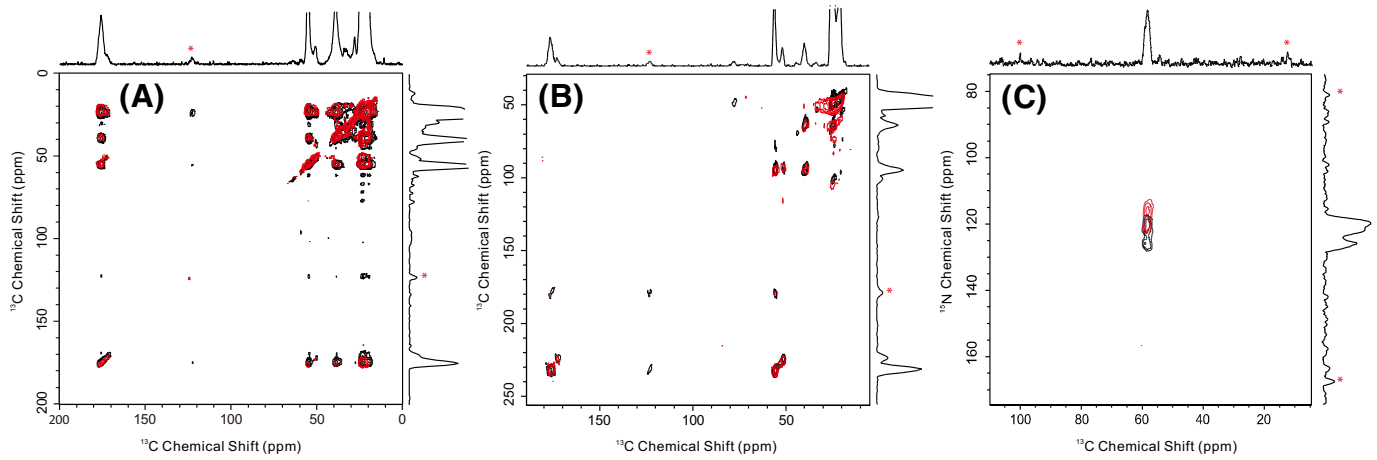


**Fig. 6.** Superimposed contours of 2D solid-state NMR experiments of [$^{13}C_9$,$^{15}N$]-Leu labeled native AR4 (black) and recombinant AR4 (red). 2D PDSD $^{13}C$–$^{13}C$ of correlation experiments (A). 2D DQ/SQ $^{13}C$–$^{13}C$ correlation experiments (B). 2D DCP $^{13}C$–$^{15}N$ correlation experiments (C). The projections for both $t_1$ and $t_2$ dimensions to the 2D spectra are also shown along with the counter map, and the spinning sidebands are indicated with red stars.

neutral pH, but native AR4 and *b*AR have almost identical time constants of M-decay (Table S1). Hence, all these observations suggest that *b*AR is more likely to assemble in trimers in the cell membrane, however, a clear measurement by AFM is required in the future.

Recombinant AR4 possesses the same temporal order of proton release and uptake compared to the native protein. Besides, when FTIR spectra of native and recombinant AR4 are compared, no shifting of predominant peaks is found, suggesting that the secondary structures of these two proteins do not change markedly. However, AR4-xz515 and *b*AR still differ in photokinetics: (i) the last component of the recovery to the ground state occurs 20 times faster in AR4-xz515 than in *b*AR (Table 1). (ii) There exists an apparent ultrafast decay before O-formation in *b*AR like that in BR, which is hardly detectable in AR4-xz515. Unfortunately, the time constants of the initial decay of O-state in BR and *b*AR are not resolved by our instrument, since it changes in the microsecond time domain [33].

The different photokinetics between *b*AR and AR4-xz515 are supposed to be caused by two factors. Firstly, AR4 aggregates in a 2D hexagonal array of trimers in the claret membrane [88], which makes it very stable even at room temperature (Table S2). Meanwhile, the bacterioruberin would also facilitate the stability of the trimeric structure of native AR4 according to the studies that bacterioruberin is suggested to play a striking role for the trimerization of AR2 [27]. But the *b*AR assembly contains no bacterioruberin, and it shows a lower stability (Table S2 and Fig. S9). Secondly, the reconstitution of archaeal rhodopsins with detergent or exogenous lipids disturbs their photokinetics in various degrees [90,91], which suggests that a natural lipid environment is important for archaeal rhodopsin to maintain its native structure and function [92–95]. The lipid environments of the host, strain L33, is thought to facilitate the protein folding of recombinant AR4 since both *xz515* and L33 are halophilic Archaea. However, the chemical nature of lipids in *xz515* has so far not been identified. The potential difference in lipid species may disturb the photokinetics between AR4-xz515 and *b*AR, as well as trimer stability, as shown for BR [96].

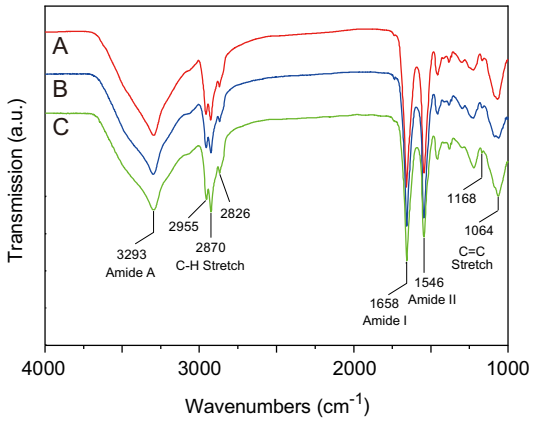


**Fig. 7.** Comparison of FTIR spectra recorded at 4 cm$^{-1}$ spectral resolution for BR (A), AR4-xz515 (B) and *b*AR (C) in 2 mM PBS at pH 7.0, 25 °C.

### 4.3. Function role of bacterioruberin and trimeric packing

The major difference between recombinant and native AR4 is the absence of bacterioruberin in the *b*AR membrane. However, the experimental results by light-induced kinetic and UV–VIS measurements show that the recombinant AR4 retains the light-driven proton pump characteristics and photo-cycling kinetics, similar to the native membrane, which indicates that a monomer is the functional unit for the protein, and in reconstitution studies of AR4 into liposomes, a similar conclusion was reached [26]. Similarly, although BR 2D crystal has a trimeric form in the purple membrane, a monomer itself is the functional unit for proton pumping [97].

The crystal structure of bacterioruberin-contained AR2 shows that the bacterioruberin binds to the crevices between each subunit of the trimer, resulting in a more compact packing form than the structure without bacterioruberin [27]. 2D DARR and DQ/SQ results show clearly that the CO peaks of the Leu residues from AR4 have spinning sidebands due to a relatively large chemical shift anisotropy, indicating that the seven helices are relatively less dynamic than those from the recombinant AR4. This may attribute to a relatively loose trimeric packing of the recombinant AR4 due to the absence of bacterioruberin. This argument is also confirmed by the DLS experiments, as shown in Fig. 8 and Table 2. A relative broad distribution of *b*AR membrane suggests a less compacted protein assembling. Thus, we can conclude that the functional role of bacterioruberin in the claret membrane is maintaining native AR4 in a more compact trimeric form, and the absence of

**Table 2**
Average particle size and polydispersity index of native and recombinant AR4 membrane fragments.

| Sample name | Average particle size (nm) | Polydispersity index |
|---|---|---|
| AR4-xz515 | 323.9 ± 2.7 | 0.155 ± 0.0106 |
| *b*AR | 261.3 ± 1.9 | 0.315 ± 0.0202 |

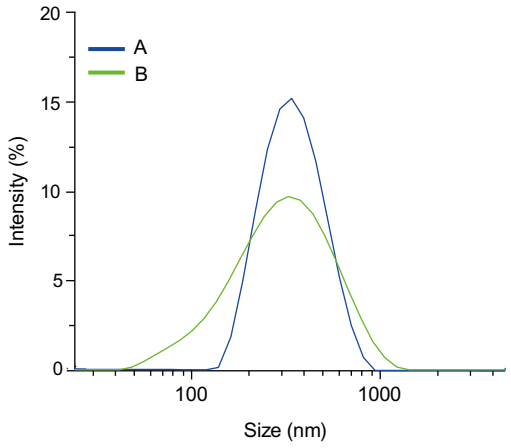


**Fig. 8.** Intensity particle size distribution of claret membrane fragments (A) and *b*AR membrane fragments (B). Nine sets of data were collected to get an average value in our experiment. However, only one set of figure was displayed since we could not offer the averaged curve.

bacterioruberin in recombinant AR4 does not affect its function, but may make the trimer structure less compact.

## 5. Conclusions

In summary, the recombinant AR4 has been functionally expressed in *H. salinarum* L33 membrane. It has several advantages over the *E. coli* expression system, a natural lipid environment, an endogenous ligand retinal, a simple purification procedure, and a high yield of 20 mg/l. Functional assay results show that the recombinant AR4 retains the light-driven proton pump characteristics and photo-cycling kinetics, similar to natural AR4 in the native membrane. The absence of bacterioruberin in recombinant AR4 trimer may not alter the protein functions but result in a less compacted trimeric assembling than natural AR4 in the native claret membrane. The stable expression system reported in this paper could pave the way for 3D structure determination and proton pumping mechanism study of AR4. It could also be applied to any other bacterial rhodopsin family members for structure–function relationship analyses in general. In addition, this work may draw attention for the further study of why bacterioruberin, or this type of carotenoid, could be synthesized in the membrane of *H. salinarum*, such as S9 or R1M1, but could not participate the trimeric packing [98].

## Transparency document

The Transparency document associated with this article can be found in the online version.

## Acknowledgements

This work has been supported financially by the NSFC (30970657, 21475045), SPP (09PJ1404300), and ECNU (79003A29, 79301207, 79301411, and 41500-515430-14100) to XZ, and by the HFERP-SAFEA (GDW20123100086) to AW. Professor Shenglin Wang from the Beijing NMR center is acknowledged for kindly providing the 3.2 mm Efree probe for us to run the DCP experiments on their 600 WB spectrometer.

## Appendix A. Supplementary data

Supplementary data to this article can be found online at http://dx.doi.org/10.1016/j.bbabio.2014.12.008.

## References

[1] D. Oesterhelt, W. Stoeckenius, Rhodopsin-like protein from the purple membrane of *Halobacterium halobium*, Nat. New Biol. 233 (1971) 149–152.
[2] Y. Mukohata, Y. Sugiyama, K. Ihara, M. Yoshida, An Australian halobacterium contains a novel proton pump retinal protein: archaerhodopsin, Biochem. Biophys. Res. Commun. 151 (1988) 1339–1345.
[3] A. Matsuno-Yagi, Y. Mukohata, Two possible roles of bacteriorhodopsin; a comparative study of strains of *Halobacterium halobium* differing in pigmentation, Biochem. Biophys. Res. Commun. 78 (1977) 237–243.
[4] O. Beja, L. Aravind, E.V. Koonin, M.T. Suzuki, A. Hadd, L.P. Nguyen, S.B. Jovanovich, C.M. Gates, R.A. Feldman, J.L. Spudich, E.N. Spudich, E.F. DeLong, Bacterial rhodopsin: evidence for a new type of phototrophy in the sea, Science 289 (2000) 1902–1906.
[5] R.A. Bogomolni, J.L. Spudich, Identification of a third rhodopsin-like pigment in phototactic *Halobacterium halobium*, Proc. Natl. Acad. Sci. U. S. A. 79 (1982) 6250–6254.
[6] S.P. Balashov, E.S. Imasheva, V.A. Boichenko, J. Anton, J.M. Wang, J.K. Lanyi, Xanthorhodopsin: a proton pump with a light-harvesting carotenoid antenna, Science 309 (2005) 2061–2064.
[7] D. Oesterhelt, The structure and mechanism of the family of retinal proteins from halophilic archaea, Curr. Opin. Struct. Biol. 8 (1998) 489–500.
[8] K. Inoue, H. Ono, R. Abe-Yoshizumi, S. Yoshizawa, H. Ito, K. Kogure, H. Kandori, A light-driven sodium ion pump in marine bacteria, Nat. Commun. 4 (2013) 1678.
[9] H.E. Kato, F. Zhang, O. Yizhar, C. Ramakrishnan, T. Nishizawa, K. Hirata, J. Ito, Y. Aita, T. Tsukazaki, S. Hayashi, P. Hegemann, A.D. Maturana, R. Ishitani, K. Deisseroth, O. Nureki, Crystal structure of the channelrhodopsin light-gated cation channel, Nature 482 (2012) 369–374.
[10] S. Reckel, D. Gottstein, J. Stehle, F. Lohr, M.K. Verhoefen, M. Takeda, R. Silvers, M. Kainosho, C. Glaubitz, J. Wachtveitl, F. Bernhard, H. Schwalbe, P. Guntert, V. Dotsch, Solution NMR structure of proteorhodopsin, Angew. Chem. Int. Ed. Engl. 50 (2011) 11942–11946.
[11] T. Kouyama, S. Kanada, Y. Takeguchi, A. Narusawa, M. Murakami, K. Ihara, Crystal structure of the light-driven chloride pump halorhodopsin from *Natronomonas pharaonis*, J. Mol. Biol. 396 (2010) 564–579.
[12] L. Pardo, J.A. Ballesteros, R. Osman, H. Weinstein, On the use of the transmembrane domain of bacteriorhodopsin as a template for modeling the three-dimensional structure of guanine nucleotide-binding regulatory protein-coupled receptors, Proc. Natl. Acad. Sci. U. S. A. 89 (1992) 4009–4012.
[13] Y. Shen, C.R. Safinya, K.S. Liang, A.F. Ruppert, K.J. Rothschild, Stabilization of the membrane protein bacteriorhodopsin to 140 °C in two-dimensional films, Nature 366 (1993) 48–50.
[14] J. Cladera, M.L. Galisteo, M. SabÉS, P.L. Mateo, E. PadrÓS, The role of retinal in the thermal stability of the purple membrane, Eur. J. Biochem. 207 (1992) 581–585.
[15] Y. Sugiyama, M. Maeda, M. Futai, Y. Mukohata, Isolation of a gene that encodes a new retinal protein, archaerhodopsin, from *Halobacterium* sp. aus-1, J. Biol. Chem. 264 (1989) 20859–20862.
[16] K. Uegaki, Y. Sugiyama, Y. Mukohata, Archaerhodopsin-2, from *Halobacterium* sp. aus-2 further reveals essential amino acid residues for light-driven proton pumps, Arch. Biochem. Biophys. 286 (1991) 107–110.
[17] K. Ihara, T. Umemura, I. Katagiri, T. Kitajima-Ihara, Y. Sugiyama, Y. Kimura, Y. Mukohata, Evolution of the archaeal rhodopsins: evolution rate changes by gene duplication and functional differentiation, J. Mol. Biol. 285 (1999) 163–174.
[18] Q. Li, Q. Sun, W. Zhao, H. Wang, D. Xu, Newly isolated archaerhodopsin from a strain of Chinese halobacteria and its proton pumping behavior, Biochim. Biophys. Acta 1466 (2000) 260–266.
[19] Q. Li, H. Wang, D. Song, W. Zhao, D. Xu, W. Huang, The isolation and purification of archaerhodopsin from *Halobacterium* sp. xz515, Acta Biochim. Biophys. Sin. 29 (1997) 517–520.
[20] Q. Li, Y. Zhang, S. Chen, J. Huang, D. Xu, J. Zhang, The detection of retinal protein similar to bacteriorhodopsin in four *Halobacterium* species, Acta Biophys. Sin. 9 (1993) 288–292.
[21] H. Wang, S. Zhan, Q. Sun, D. Xu, W. Zhao, W. Huang, Q. Li, Primary structure of helix C to helix G of a new retinal protein in H.sp.xz515, Chin. Sci. Bull. 45 (2000) 1108–1113.
[22] Y. Wang, D. Ma, Y. Zhao, M. Ming, J. Wu, J. Ding, Light-driven proton pumps of archaerhodopsin and bacteriorhodopsin & polymer-matrix composite materials of those functional proteins, Acta Polym. Sin. (2012) 698–713.
[23] M. Ming, M. Lu, S.P. Balashov, T.G. Ebrey, Q. Li, J. Ding, pH dependence of light-driven proton pumping by an archaerhodopsin from Tibet: comparison with bacteriorhodopsin, Biophys. J. 90 (2006) 3322–3332.
[24] M. Ming, Y. Wang, J. Wu, D. Ma, Q. Li, J. Ding, Triton X-100 can alter the temporal sequence of the light-driven proton pump of archaerhodopsin 4, FEBS Lett. 580 (2006) 6749–6753.
[25] W. Zhao, M. Chai, F. Hai, D. Xu, Q. Li, Photochemical and proton pumping properties of archaerhodopsin in halobacteria H. sp. xz515, Acta Biophys. Sin. 14 (1998) 543–547.
[26] J. Wu, L. Huang, J. Liu, M. Ming, Q.-G. Li, J.-D. Ding, Directional self-assembly in archaerhodopsin-reconstituted phospholipid liposomes, Chin. J. Chem. 23 (2005) 330–333.
[27] K. Yoshimura, T. Kouyama, Structural role of bacterioruberin in the trimeric structure of archaerhodopsin-2, J. Mol. Biol. 375 (2008) 1267–1281.
[28] J. Wu, D. Ma, Y. Wang, M. Ming, S.P. Balashov, J. Ding, Efficient approach to determine the pKa of the proton release complex in the photocycle of retinal proteins, J. Phys. Chem. B 113 (2009) 4482–4491.
[29] F. Bernaudat, A. Frelet-Barrand, N. Pochon, S. Dementin, P. Hivin, S. Boutigny, J.B. Rioux, D. Salvi, D. Seigneurin-Berny, P. Richaud, J. Joyard, D. Pignol, M. Sabaty, T. Desnos, E. Pebay-Peyroula, E. Darrouzet, T. Vernet, N. Rolland, Heterologous expression of membrane proteins: choosing the appropriate host, PLoS ONE 6 (2011) e29191.

[30] E.C. Saint Clair, J.I. Ogren, S. Mamaev, J.M. Kralj, K.J. Rothschild, Conformational changes in the archaerhodopsin-3 proton pump: detection of conserved strongly hydrogen bonded water networks, J. Biol. Phys. 38 (2012) 153–168.
[31] E.C. Saint Clair, J.I. Ogren, S. Mamaev, D. Russano, J.M. Kralj, K.J. Rothschild, Near-IR resonance Raman spectroscopy of archaerhodopsin 3: effects of transmembrane potential, J. Phys. Chem. B 116 (2012) 14592–14601.
[32] G. Schmies, I. Chizhov, M. Engelhard, Functional expression of His-tagged sensory rhodopsin I in *Escherichia coli*, FEBS Lett. 466 (2000) 67–69.
[33] I.P. Hohenfeld, A.A. Wegener, M. Engelhard, Purification of histidine tagged bacteriorhodopsin, pharaonis halorhodopsin and pharaonis sensory rhodopsin II functionally expressed in *Escherichia coli*, FEBS Lett. 442 (1999) 198–202.
[34] J.W.H. Weijers, S. Schouten, E.C. Hopmans, J.A.J. Geenevasen, O.R.P. David, J.M. Coleman, R.D. Pancost, J.S. Sinninghe Damsté, Membrane lipids of mesophilic anaerobic bacteria thriving in peats have typical archaeal traits, Environ. Microbiol. 8 (2006) 648–657.
[35] B.F. Ni, M. Chang, A. Duschl, J. Lanyi, R. Needleman, An efficient system for the synthesis of bacteriorhodopsin in *Halobacterium halobium*, Gene 90 (1990) 169–172.
[36] Y. Wang, J. Hong, M. Ming, J. Ding, Q. Li, W. Huang, Rapid cloning of an archaerhodopsin gene from *Halobacterium* species xz515 by LPA, J. Fudan Univ. 42 (2003) 576–583.
[37] D. Oesterhelt, W. Stoeckenius, Isolation of the cell membrane of *Halobacterium halobium* and its fractionation into red and purple membrane, Methods Enzymol. 31 (1974) 667–678.
[38] S.L. Helgerson, S.L. Siemsen, E.A. Dratz, Enrichment of bacteriorhodopsin with isotopically labeled amino acids by biosynthetic incorporation in *Halobacterium halobium*, Can. J. Microbiol. 38 (1992) 1181–1185.
[39] Y. Wang, Y. Zhao, M. Ming, J. Wu, W. Huang, J. Ding, Effect of substitution of proline-77 to aspartate on the light-driven proton release of bacteriorhodopsin, Photochem. Photobiol. 88 (2012) 922–927.
[40] G. Metz, X.L. Wu, S.O. Smith, Ramped-amplitude cross polarization in magic-angle-spinning NMR, J. Magn. Reson. Ser. A 110 (1994) 219–227.
[41] S. Hediger, B.H. Meier, R.R. Ernst, Adiabatic passage Hartmann–Hahn cross polarization in NMR under magic angle sample spinning, Chem. Phys. Lett. 240 (1995) 449–456.
[42] A.E. Bennett, C.M. Rienstra, M. Auger, K.V. Lakshmi, R.G. Griffin, Heteronuclear decoupling in rotating solids, J. Chem. Phys. 103 (1995) 6951–6958.
[43] C.R. Morcombe, K.W. Zilm, Chemical shift referencing in MAS solid state NMR, J. Magn. Reson. 162 (2003) 479–486.
[44] N.M. Szeverenyi, M.J. Sullivan, G.E. Maciel, Observation of spin exchange by two-dimensional Fourier transform $^{13}C$ cross polarization-magic-angle spinning, J. Magn. Reson. 47 (1982) 462–475.
[45] K. Takegoshi, S. Nakamura, T. Terao, $^{13}C$–$^{1}H$ dipolar-assisted rotational resonance in magic-angle spinning NMR, Chem. Phys. Lett. 344 (2001) 631–637.
[46] M.H. Levitt, Symmetry-based Pulse Sequences in Magic-angle Spinning Solid-state NMR, eMagRes, John Wiley & Sons, Ltd., 2007
[47] M. Hohwy, H.J. Jakobsen, M. Eden, M.H. Levitt, N.C. Nielsen, Broadband dipolar recoupling in the nuclear magnetic resonance of rotating solids: a compensated C7 pulse sequence, J. Chem. Phys. 108 (1998) 2686–2694.
[48] V. Ladizhansky, S. Vega, Polarization transfer dynamics in Lee–Goldburg cross polarization nuclear magnetic resonance experiments on rotating solids, J. Chem. Phys. 112 (2000) 7158–7168.
[49] J. Schaefer, R.A. McKay, E.O. Stejskal, Double-cross-polarization NMR of solids, J. Magn. Reson. 34 (1979) 443–447.
[50] M.B. Gochnauer, D.J. Kushner, Growth and nutrition of extremely halophilic bacteria, Can. J. Microbiol. 15 (1969) 1157–1165.
[51] M.M. Bradford, A rapid and sensitive method for the quantitation of microgram quantities of protein utilizing the principle of protein–dye binding, Anal. Biochem. 72 (1976) 248–254.
[52] R.F. Shand, M.C. Betlach, Expression of the *bop* gene cluster of *Halobacterium halobium* is induced by low oxygen tension and by light, J. Bacteriol. 173 (1991) 4692–4699.
[53] W. Wang, Z. Nossoni, T. Berbasova, C.T. Watson, I. Yapici, K.S. Lee, C. Vasileiou, J.H. Geiger, B. Borhan, Tuning the electronic absorption of protein-embedded all-trans-retinal, Science 338 (2012) 1340–1343.
[54] P.J.R. Spooner, J.M. Sharples, S.C. Goodall, P.H.M. Bovee-Geurts, M.A. Verhoeven, J. Lugtenburg, A.M.A. Pistorius, W.J. DeGrip, A. Watts, The ring of the rhodopsin chromophore in a hydrophobic activation switch within the binding pocket, J. Mol. Biol. 343 (2004) 719–730.
[55] S.C. Kushwaha, M. Kates, Studies of the biosynthesis of C50 carotenoids in *Halobacterium cutirubrum*, Can. J. Microbiol. 25 (1979) 1292–1297.
[56] I. Dundas, H. Larsen, The physiological role of the carotenoid pigments of *Halobacterium salinarium*, Arch. Mikrobiol. 44 (1962) 233–239.
[57] J. Ding, Discovery, investigation and application of archaea rhodopsin 4, The 13th Chinese and International Biophysics Congress, Nanchang, Jiangxi, China, 2013, pp. 03–008.
[58] Y.K. Lee, N.D. Kurur, M. Helmle, O.G. Johannessen, N.C. Nielsen, M.H. Levitt, Efficient dipolar recoupling in the NMR of rotating solids. A sevenfold symmetric radiofrequency pulse sequence, Chem. Phys. Lett. 242 (1995) 304–309.
[59] A. Brinkmann, M. Eden, M.H. Levitt, Synchronous helical pulse sequences in magic-angle spinning nuclear magnetic resonance: double quantum recoupling of multiple-spin systems, J. Chem. Phys. 112 (2000) 8539–8554.
[60] M. Carravetta, M. Eden, X. Zhao, A. Brinkmann, M.H. Levitt, Symmetry principles for the design of radiofrequency pulse sequences in the nuclear magnetic resonance of rotating solids, Chem. Phys. Lett. 321 (2000) 205–215.
[61] M.H. Levitt, Symmetry-based pulse sequences in magic-angle spinning solid-state NMR, in: D.M. Grant, R.K. Harris (Eds.), Encyclopedia of Nuclear Magnetic Resonance, John Wiley & Sons, Ltd, Chichester, UK, 2002.
[62] S. Wang, R.A. Munro, L. Shi, I. Kawamura, T. Okitsu, A. Wada, S.-Y. Kim, K.-H. Jung, L.S. Brown, V. Ladizhansky, Solid-state NMR spectroscopy structure determination of a lipid-embedded heptahelical membrane protein, Nat. Methods 10 (2013) 1007–1012.
[63] I.A. Grabchuk, V.Y. Orekhov, A.S. Arseniev, $^{1}H$–$^{15}N$ backbone resonance assignments of bacteriorhodopsin, Pharm. Acta Helv. 71 (1996) 97–102.
[64] L. Shi, M.A. Ahmed, W. Zhang, G. Whited, L.S. Brown, V. Ladizhansky, Three-dimensional solid-state NMR study of a seven-helical integral membrane proton pump — structural insights, J. Mol. Biol. 386 (2009) 1078–1093.
[65] L. Shi, I. Kawamura, K.-H. Jung, L.S. Brown, V. Ladizhansky, Conformation of a seven-helical transmembrane photosensor in the lipid environment, Angew. Chem. Int. Ed. Engl. 50 (2011) 1302–1305.
[66] V.A. Higman, K. Varga, L. Aslimovska, P.J. Judge, L.J. Sperling, C.M. Rienstra, A. Watts, The conformation of bacteriorhodopsin loops in purple membranes resolved by solid-state MAS NMR spectroscopy, Angew. Chem. Int. Ed. Engl. 50 (2011) 8432–8435.
[67] H. Luecke, B. Schobert, H.T. Richter, J.P. Cartailler, J.K. Lanyi, Structural changes in bacteriorhodopsin during ion transport at 2 angstrom resolution, Science 286 (1999) 255–260.
[68] H. Luecke, B. Schobert, H.T. Richter, J.P. Cartailler, J.K. Lanyi, Structure of bacteriorhodopsin at 1.55 Å resolution, J. Mol. Biol. 291 (1999) 899–911.
[69] X. Zhao, Protein structure determination by solid-state NMR, Top. Curr. Chem. 326 (2012) 187–213.
[70] A. Watts, S.K. Straus, S.L. Grage, M. Kamihira, Y.H. Lam, X. Zhao, Membrane protein structure determination using solid-state NMR, in: A.K. Downing (Ed.), Methods in Molecular Biology: Protein NMR Techniques, Humana Press Inc., Totowa, NJ, 2004, pp. 403–473.
[71] T. Vosegaard, M. Kamihira-Ishijima, A. Watts, N.C. Nielsen, Helix conformations in 7TM membrane proteins determined using oriented-sample solid-state NMR with multiple residue-specific N-15 labeling, Biophys. J. 94 (2008) 241–250.
[72] M. Kamihira, A. Watts, Functionally relevant coupled dynamic profile of bacteriorhodopsin and lipids in purple membranes, Biochemistry 45 (2006) 4304–4313.
[73] M. Kamihira, T. Vosegaard, A.J. Mason, S.K. Straus, N.C. Nielsen, A. Watts, Structural and orientational constraints of bacteriorhodopsin in purple membranes determined by oriented-sample solid-state NMR spectroscopy, J. Struct. Biol. 149 (2005) 7–16.
[74] C. Glaubitz, I.J. Burnett, G. Gröbner, A.J. Mason, A. Watts, Deuterium-MAS NMR spectroscopy on oriented membrane proteins: applications to photointermediates of bacteriorhodopsin, J. Am. Chem. Soc. 121 (1999) 5787–5794.
[75] X. Ding, X. Zhao, A. Watts, G-protein-coupled receptor structure, ligand binding and activation as studied by solid-state NMR spectroscopy, Biochem. J. 450 (2013) 443–457.
[76] X. Ding, Z. Cao, Y. Li, L. Xie, X. Zhao, Spectroscopic studies of 7TM retinal proteins, The 13th Chinese and International Biophysics Congress, Nanchang, Jiangxi, China, 2013 pp. 08–012.
[77] S.O. Smith, J. Lugtenburg, R.A. Mathies, Determination of retinal chromophore structure in bacteriorhodopsin with resonance Raman spectroscopy, J. Membr. Biol. 85 (1985) 95–109.
[78] S.O. Smith, M.S. Braiman, A.B. Myers, J.A. Pardoen, J.M.L. Courtin, C. Winkel, J. Lugtenburg, R.A. Mathies, Vibrational analysis of the all-*trans*-retinal chromophore in light-adapted bacteriorhodopsin, J. Am. Chem. Soc. 109 (1987) 3108–3125.
[79] Y. Fan, L. Shi, V. Ladizhansky, L. Brown, Uniform isotope labeling of a eukaryotic seven-transmembrane helical protein in yeast enables high-resolution solid-state NMR studies in the lipid environment, J. Biomol. NMR 49 (2011) 151–161.
[80] Y. Zhao, Effect of Mutagenesis on Functions of Bacteriorhodopsin and Corresponding Protein-based Functional Materials, Department of Macromolecular Science, Fundan University, Shanghai, 2010. pp. 120–134.
[81] J. Zhang, K. Mizuno, Y. Murata, H. Koide, M. Murakami, K. Ihara, T. Kouyama, Crystal structure of deltarhodopsin-3 from *Haloterrigena thermotolerans*, Proteins, (2013).
[82] M. Kamekura, Y. Seno, H. Tomioka, Detection and expression of a gene encoding a new bacteriorhodopsin from an extreme halophile strain HT (JCM 9743) which does not possess bacteriorhodopsin activity, Extremophiles 2 (1998) 33–39.
[83] R. Dunn, J. McCoy, M. Simsek, A. Majumdar, S.H. Chang, U.L. RajBhandary, H.G. Khorana, The bacteriorhodopsin gene, Proc. Natl. Acad. Sci. U. S. A. 78 (1981) 6744–6748.
[84] S. Dassarma, U.L. Rajbhandary, H.G. Khorana, Bacterio-opsin mRNA in wild-type and bacterio-opsin-deficient *Halobacterium halobium* strains, Proc. Natl. Acad. Sci. U. S. A. 81 (1984) 125–129.
[85] Z.J. Xu, D.B. Moffett, T.R. Peters, L.D. Smith, B.P. Perry, J. Whitmer, S.A. Stokke, M. Teintze, The role of the leader sequence coding region in expression and assembly of bacteriorhodopsin, J. Biol. Chem. 270 (1995) 24858–24863.
[86] O. Gonzalez, S. Gronau, M. Falb, F. Pfeiffer, E. Mendoza, R. Zimmer, D. Oesterhelt, Reconstruction, modeling & analysis of *Halobacterium salinarum* R-1 metabolism, Mol. Biosyst. 4 (2008) 148–159.
[87] M. Falb, K. Müller, L. Königsmaier, T. Oberwinkler, P. Horn, S. von Gronau, O. Gonzalez, F. Pfeiffer, E. Bornberg-Bauer, D. Oesterhelt, Metabolism of halophilic archaea, Extremophiles 12 (2008) 177–196.
[88] L. Tang, Q.A. Sun, Q. Li, Y. Huang, Q. Wei, Y. Zhang, J. Hu, Z. Zhang, M. Li, F. Yang, Imaging bacteriorhodopsin-like molecules of claret-membranes from Tibet halobacteria xz515 by atomic force microscope, Chin. Sci. Bull. 46 (2001) 1897–1900.
[89] Y. Wang, J. Wu, M. Ming, Y. Zhao, J. Ding, Effects of Triton X-100 on proton transfer and in the photocycle of archaerhodopsin 4, Biosci. Biotechnol. Biochem. 76 (2012) 250–256.

[90] M.K. Joshi, S. Dracheva, A.K. Mukhopadhyay, S. Bose, R.W. Hendler, Importance of specific native lipids in controlling the photocycle of bacteriorhodopsin, Biochemistry 37 (1998) 14463–14470.
[91] S.J. Milder, T.E. Thorgeirsson, L.J. Miercke, R.M. Stroud, D.S. Kliger, Effects of detergent environments on the photocycle of purified monomeric bacteriorhodopsin, Biochemistry 30 (1991) 1751–1761.
[92] J.P. Cartailler, H. Luecke, X-ray crystallographic analysis of lipid–protein interactions in the bacteriorhodopsin purple membrane, Annu. Rev. Biophys. Biomol. Struct. 32 (2003) 285–310.
[93] R.W. Hendler, S.M. Barnett, S. Dracheva, S. Bose, I.W. Levin, Purple membrane lipid control of bacteriorhodopsin conformational flexibility and photocycle activity — an infrared spectroscopic study, Eur. J. Biochem. 270 (2003) 1920–1925.
[94] R.W. Hendler, S. Dracheva, Importance of lipids for bacteriorhodopsin structure, photocycle, and function, Biochemistry (Mosc) 66 (2001) 1311–1314.
[95] K. Hu, Y. Sun, D. Chen, Y. Zhang, The effect of lipid environment in purple membrane on bacteriorhodopsin, J. Photochem. Photobiol. B 58 (2000) 163–169.
[96] B. Sternberg, P. Gale, A. Watts, The effect of temperature and protein content on the dispersive properties of bacteriorhodopsin from *H. halobium* in reconstituted DMPC complexes free of endogenous purple membrane lipids: a freeze-fracture electron microscopy study, Biochim. Biophys. Acta Biomembr. 980 (1989) 117–126.
[97] N.A. Dencher, H.J. Sass, G. Büldt, Water and bacteriorhodopsin: structure, dynamics, and function, Biochim. Biophys. Acta 1460 (2000) 192–203.
[98] A.M. Dummer, J.C. Bonsall, J.B. Cihla, S.M. Lawry, G.C. Johnson, R.F. Peck, Bacterioopsin-mediated regulation of bacterioruberin biosynthesis in *Halobacterium salinarum*, J. Bacteriol. 193 (2011) 5658–5667.